J Mater Sci: Mater Med
DOI 10.1007/s10856-013-5101-4

Bone bonding ability of a chemically and thermally treated low elastic modulus Ti alloy: gum metal

Masashi Tanaka · Mitsuru Takemoto · Shunsuke Fujibayashi · Toshiyuki Kawai · Seiji Yamaguchi · Takashi Kizuki · Tomiharu Matsushita · Tadashi Kokubo · Takashi Nakamura · Shuichi Matsuda

Received: 25 September 2013 / Accepted: 17 November 2013

Abstract The gum metal with composition Ti–36Nb–2Ta–3Zr–0.3O, is free from cytotoxic elements and exhibits a low elastic modulus as well as high mechanical strength. We have previously demonstrated that this gum metal, once subjected to a series of surface treatments—immersion in 1 M NaOH (alkali treatment) and then 100 mM $CaCl_2$, before heating at 700 °C (sample: ACaH-GM), with an optional final hot water immersion (sample: ACaHW-GM)—has apatite-forming ability in simulated body fluid. To confirm the in vivo bioactivity of these treated alloys, failure loads between implants and bone at 4, 8, 16, and 26 weeks after implantation in rabbits' tibiae were measured for untreated gum metal (UT-GM), ACaH-GM and ACaHW-GM, as well as pure titanium plates after alkali and heat treatment (AH-Ti). The ACaH-GM and UT-GM plates showed almost no bonding, whereas ACaHW-GM and AH-Ti plates showed successful bonding by 4 weeks, and their failure loads subsequently increased with time. The histological findings showed a large amount of new bone in contact with the surface of ACaHW-GM and AH-Ti plates, suggesting that the ACaHW treatment could impart bone-bonding bioactivity to a gum metal in vivo. Thus, with this improved bioactive treatment, these advantageous gum metals become useful candidates for orthopedic and dental devices.

M. Tanaka (✉) · M. Takemoto · S. Fujibayashi · T. Kawai · S. Matsuda
Department of Orthopaedic Surgery, Graduate School of Medicine, Kyoto University, 54 Kawahara-cho, Shougoin, Sakyou-ku, Kyoto 606-8507, Japan
e-mail: masashit@kuhp.kyoto-u.ac.jp

S. Yamaguchi · T. Kizuki · T. Matsushita · T. Kokubo
Department of Biomedical Sciences, College of Life and Health Sciences, Chubu University, 1200 Matsumoto-cho, Kasugai, Aichi 487-8501, Japan

T. Nakamura
National Hospital Organization Kyoto Medical Center, 1-1 Fukakusa Mukaihata-cho, Fushimi-ku, Kyoto 612-8555, Japan

1 Introduction

Commercially pure titanium (cp-Ti) and Ti–6Al–4V alloy are commercially available and currently used as biomaterials for bone plates, intramedullary nails, and the artificial joints of total hip arthroplasties because they have excellent specific corrosion resistance, do not cause allergic reactions and, for metallic biomaterials, show good biocompatibility with bone [1]. Among them, Ti–6Al–4V alloy has been widely used in orthopedics [2], because it has excellent specific strength when compared with that of cp-Ti. However, the Young's modulus of Ti–6Al–4V alloy (110 GPa) is much greater than that of human cortical bone (10–30 GPa) [3], so the stems of cementless total hip arthroplasties made with high Young's modulus alloys sometimes cause severe stress shielding in the femur, leading to thigh pain when walking [4–6]. To solve these problems, so-called 'isoelastic stems' which have similar elastic modulus to human cortical bone were developed in the 1980s; these were aimed at providing a more natural stress distribution in the proximal femur, in the hope of reducing stress shielding [7–9].

In 2003, Saito et al. [10] reported that Ti–36Nb–2Ta–3Zr–0.3O alloy showed certain favorable mechanical properties such as low Young's modulus (55 GPa) and high mechanical strength (1,200 MPa), as well as a capacity for extensive elastic deformation and clayey plasticity; this alloy (and related alloys) were named 'gum metal', because of their mechanical characteristics. Gum

Published online: 29 November 2013

metals are used commercially as wires for orthodontics, and in the frames of glasses or shafts of golf clubs, but they are not yet used as biomaterials for orthopedic or dental implant applications.

In 2012, Yamaguchi et al. [11] reported that the gum metal with composition Ti–36Nb–2Ta–3Zr–0.3O exhibited a high capacity for apatite formation in a simulated body fluid (SBF) once subjected to a series of treatments: immersion in 1 M NaOH (alkali treatment) and then 100 mM $CaCl_2$ treatment, heating at 700 °C, followed by immersion in hot water (ACaHW treatment, to give ACaHW-GM). The high-apatite formation was attributed to the $CaTi_2O_5$ that was precipitated on the surface, and found to be maintained, even in a humid environment, over a long period. On the other hand, without the hot water step in the surface treatment process, this gum metal (ACaH-GM) did not exhibit any capacity for apatite formation in SBF. Surface structures after both series of treatments are similar as shown by field emission-scanning electron microscope images. The apatite-forming ability in SBF suggests a high potential for bone-bonding in the living body [12–14], which would be useful for orthopedic and dental implants. This means that we need to verify in vivo the effect of the hot water step on the osteoconductivity of ACaH-GM and ACaHW-GM.

In addition, the toxicity of V has been previously pointed out [15]. So the V in Ti–6Al–4V has been replaced by other β-stabilizing elements, such as Fe and Nb, both of which are considered to be safer than V for the living body [15].

The purpose of this study is to evaluate in vivo osteoconductivity (which is crucial for clinical applications) of a chemically and thermally treated low modulus Ti alloy: gum metal. Samples of untreated gum metal (UT-GM), two different chemically and thermally treated gum metals (ACaH-GM and ACaHW-GM) and pure titanium subjected to alkali and heat treatment (AH-Ti) were prepared for this study. In previous studies, apatite was shown to form on the surfaces of ACaHW-GM plates and AH-Ti plates after soaking in SBF for 3 days; UT-GM and ACaH-GM plates did not show any apatite-forming ability [11, 16]. If in vivo osteoconductivity is shown, these alloys may be used for bioactive cementless total hip arthroplasties, and would be expected to reduce stress shielding in the femur and consequent thigh pain.

2 Materials and methods

2.1 Implant preparation

Plates of size 15 × 10 × 2 mm were prepared from the gum metal: Ti–36Nb–2Ta–3Zr–0.3O alloy sheet (Toyota Central Research and Development Laboratories, Inc., Ti: Bal., Nb:36.39, Ta: 2.00, Zr: 2.87, O: 0.31, Fe: 0.02 mass%) and cp-Ti (Ti > 99.5 mass%). The plates were polished with a No. 400 diamond plate, then washed with acetone, 2-propanol, and ultrapure water in an ultrasonic cleaner for 30 min each, and finally dried at 40 °C.

Table 1 Types of implanted plates

Type of implant	Treatment	Apatite-forming ability in SBF
UT-GM	Untreated gum metal	No
ACaH-GM	1 M NaOH, 100 mM $CaCl_2$, and heat (700 °C) treated gum metal	No
ACaHW-GM	1 M NaOH, 100 mM $CaCl_2$, heat (700 °C) and water treated gum metal	Yes
AH-Ti	5 M NaOH and heat (600 °C) treated pure Ti	Yes

UT-GM untreated gum metal, *ACaH-GM* alkali, $CaCl_2$ and heat treated gum metal, *ACaHW-GM* alkali, $CaCl_2$, heat and water treated gum metal, and *AH-Ti* alkali and heat treated pure Ti

The plates of gum metal were first soaked in 10 mL of 1 M aqueous NaOH solution at 60 °C for 24 h (alkali treatment). After removal from the solution they were gently rinsed with ultrapure water for 30 s and dried at 40 °C. The plates were subsequently soaked in 20 mL of 100 mM $CaCl_2$ solution at 40 °C for 24 h, and then washed and dried in a similar manner. Next, they were heated to 700 °C at a rate of 5 °C min^{-1} in an electric furnace in air and kept at that temperature for 1 h, followed by natural cooling (ACaH-GM). After the heat treatment, some plates were soaked in 20 mL of ultrapure water at 80 °C for 24 h, and then washed and dried (ACaHW-GM). Apatite was shown to form on the surfaces of ACaHW-GM plates after soaking in SBF for 3 days, but ACaH-GM plates did not show any apatite-forming ability [11].

For the positive controls in the animal experiments, pure titanium plates were soaked in 5 M aqueous NaOH solution at 60 °C for 24 h (alkali treatment). After removal from the solution they were gently rinsed with ultrapure water for 30s and dried at 40 °C for 24 h in an air atmosphere. Next, they were heated to 600 °C at a rate of 5 °C min^{-1} in an electrical furnace in air and kept at that temperature for 1 h, followed by natural cooling (AH-Ti). Apatite was shown to form on the surfaces of AH-Ti plates after soaking in SBF for 3 days [16], and pure titanium after this treatment is already known to show osteoconductivity in vivo [12, 17, 18].

Untreated plates of gum metal (UT-GM) were used as negative controls in the animal experiments. UT-GM plates did not show any apatite-forming ability [11]. Thus, a total of four different types of plates were implanted (Table 1).

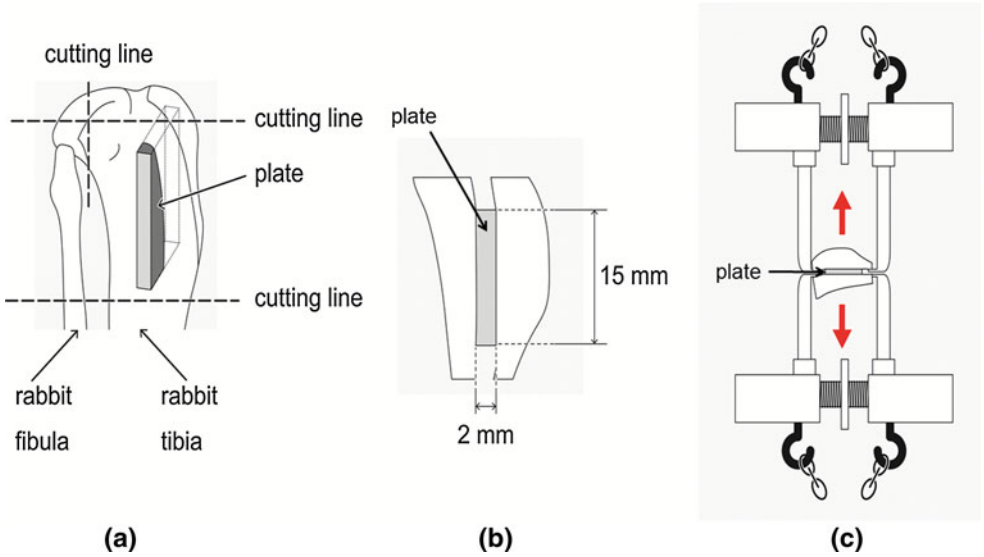

Fig. 1 Schematic drawings showing preparation of test specimens and the set-up for detaching tests. (**a**) Insertion of the titanium plate into the rabbit tibia. (**b**) The bone–plate–bone construct after cutting the tibia at the proximal and distal ends of the plate. (**c**) The anterior and posterior cortices were held, and tensile load was applied until detachment occurred

2.2 Surface analyses

The surfaces of the treated plates were analyzed by a field emission-scanning electron microscope (FE-SEM) (S-4300; Hitachi Co., Tokyo, Japan) equipped with an energy dispersive X-ray (EDX) analyzer (EMAX-7000; Horiba Ltd., Kyoto, Japan). The FE-SEM and EDX analyses were carried out at accelerating voltages of 15 and 5 kV, respectively.

2.3 Animal study

The plates were conventionally sterilized using ethylene oxide gas and implanted into the metaphyses of the tibiae of mature male Japanese white rabbits weighing 2.8–3.5 kg. The surgical methods used have been described previously [12, 17–19]. Briefly, the rabbits were anesthetized with an intravenous injection of sodium pentobarbital (0.5 mL kg^{-1}) and local administration of a solution of 0.5 % lidocaine. A 3-cm-long longitudinal skin incision was made on the medial side of the knee and the fascia and periosteum were incised and retracted to expose the tibial cortex. Using a dental burr, a 16 × 2 mm^2 hole was made from the medial to the lateral cortex running parallel to the longitudinal axis of the tibial metaphyses, as shown in Fig. 1a. After irrigating the hole with saline, the plates were implanted in the frontal direction, perforating the tibia and protruding from the medial to lateral cortex. The fascia and skin were closed in layers and the same surgical procedures were performed bilaterally.

The animals were housed individually in standard rabbit cages and fed standard rabbit food and water ad libitum. Each rabbit was euthanized with an overdose of intravenous sodium pentobarbital at 4, 8, 16, or 26 weeks after implantation; a total of 80 rabbits were used (10 plates of each type per implantation time). The Kyoto University guidelines for animal experiments were observed in this study.

2.4 Measurement of detaching failure load

After euthanasia, the segments of the proximal tibial metaphyses containing the implanted plates were harvested and eight samples were prepared for detaching tests [19]. All samples were kept moist after harvesting. The bone tissue surrounding the plates was carefully removed on both sides and at the ends; a dental burr was used to remove periosteal bone growth. Traction was applied vertically to the implant surface using load test equipment (model 1310VRW; Aikoh Engineering Co. Ltd., Nagoya, Japan) at a crosshead speed of 35 mm min^{-1} (Fig. 1b, c). Specially designed hooks held the bone-plate-bone construct. The detaching failure load was measured when the plate detached from the bone. If the plate detached before the test, then the failure load was defined as 0 N. Eight samples were analyzed for each type of implant at each implantation period.

All data were recorded as the mean ± standard deviation (SD). They were assessed using one-way analysis of variance followed by Tukey–Kramer multiple comparison post hoc tests at each time point. For statistical analysis, JMP 9 (SAS Institute, Cary, NC, USA) was used. Differences with $P < 0.05$ were considered statistically significant.

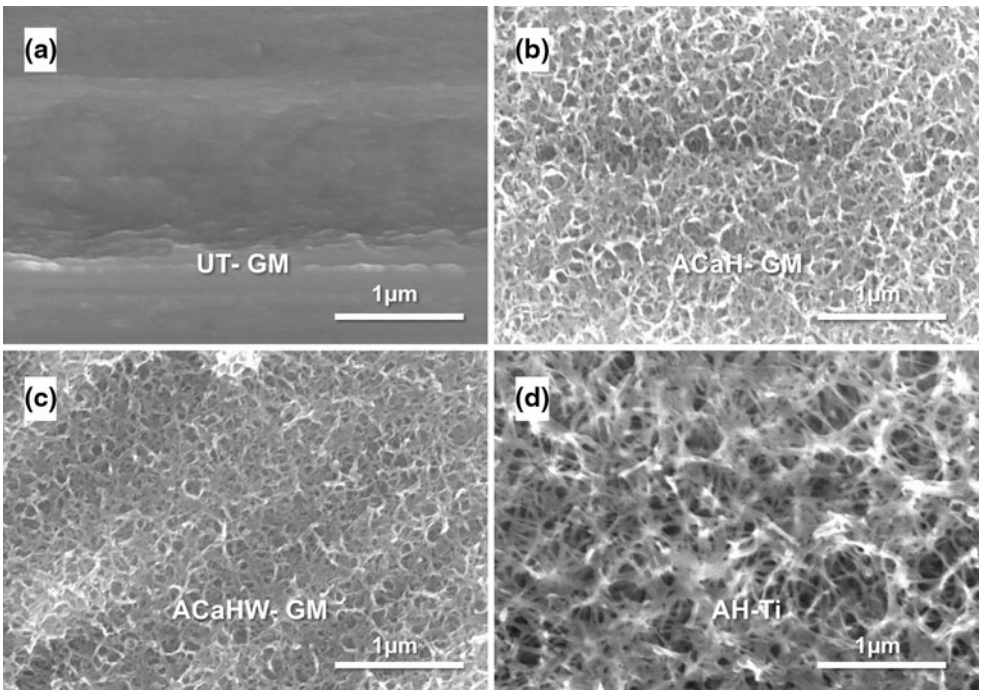

Fig. 2 FE-SEM images of the surfaces of the treated implants. (**a**) UT-GM, (**b**) ACaH-GM, (**c**) ACaHW-GM, and (**d**) AH-Ti

2.5 Histological examination

2.5.1 Surface examination after detaching test

After the detaching tests, samples from each group at each interval after implantation were separated from any soft tissue by soaking in 30 % sodium hypochlorite aqueous solution for 3 h. Subsequently, they were fixed in 10 % phosphate-buffered formalin for 3 days and dehydrated in serial concentrations of ethanol (70, 80, 90, 99, 100, and 100 vol%) for 1 day each. Then they were soaked in isopentyl acetate solution for 1 day and dried in a critical point drying apparatus (hcp-2; Hitachi Ltd., Tokyo, Japan). The samples were sputter-coated with platinum and palladium for SEM observation (S-4700; Hitachi Ltd.) and coated with carbon for SEM–EDX analyses (EMAX-7000; Horiba Ltd., Kyoto, Japan). The SEM–EDX observations were performed mainly at the sample surface.

2.5.2 Histological examination

Two specimens from each group harvested after each time interval were allocated to histological examinations. The segments of the tibiae containing the implanted samples were fixed in 10 % phosphate-buffered formalin for 7 days, and dehydrated in serial concentrations of ethanol (70, 80, 90, 99, 100, and 100 % v/v) for 3 days at each concentration. Some sections with a thickness of 500 μm were cut, bound to a transparent acrylic plate, and ground to a thickness of 40–50 μm. These samples were stained using Stevenel's blue and Van Gieson's picrofuchsin. Histological evaluation was performed on each stained section using a digital microscope (DSX 500; Olympus, Tokyo, Japan).

3 Results

3.1 In vitro evaluation

3.1.1 Surface structures

Figure 2 shows FE-SEM images of the surfaces of the implants. A fine network structure was seen at the nanometer scale on the ACaH-GM and ACaHW-GM samples, and at the submicrometer scale on the AH-Ti sample; no fine network structure was seen on the UT-GM plate.

3.2 In vivo evaluation

All rabbits tolerated the surgical procedure well. None exhibited infection of the surgical site, dislocation of the implants, or adverse reactions such as inflammation or foreign body reactions on or around the implants.

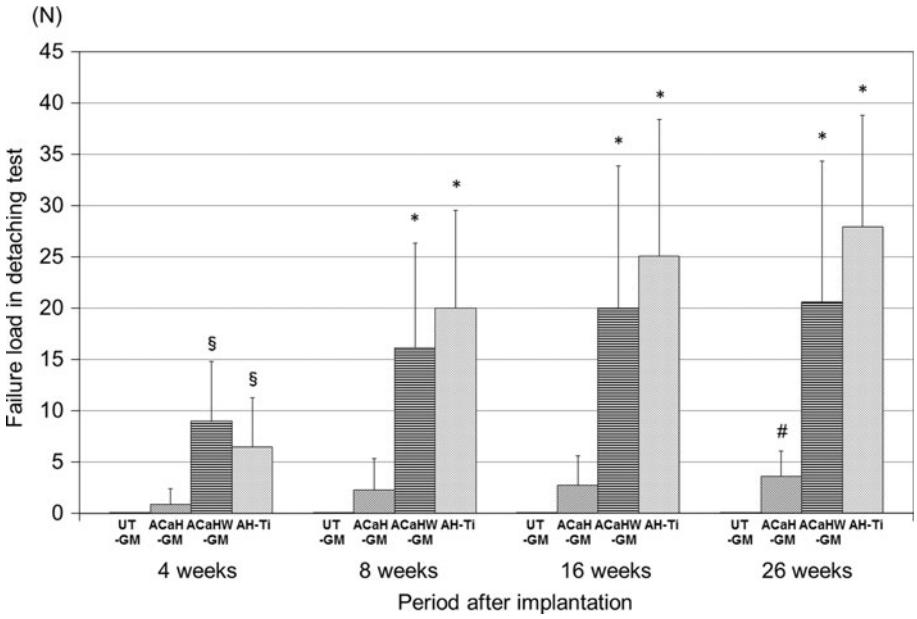

Fig. 3 Failure loads in the detaching tests at different periods after implantation for gum metals subjected to various treatments and AH-Ti. (*Error bar* standard deviation) (N). *P* values of ACaHW-GM versus UT-GM, AH-Ti versus UT-GM, ACaHW-GM versus ACaH-GM and AH-Ti versus ACaH-GM were, respectively, 0.008, 0.008, 0.0192, and 0.0364 at 4 weeks; 0.0023, 0.0023, 0.0081, and 0.0048 at 8 weeks; 0.0023, 0.0023, 0.0050, and 0.0050 at 16 weeks; 0.0023, 0.0023, 0.0052, and 0.0052 at 26 weeks. $^{*}P < 0.01$ versus UT-GM and ACaH-GM, $^{\S}P < 0.01$ versus UT-GM and $P < 0.05$ versus ACaH-GM, $^{\#}P < 0.05$ vs UT-GM

3.2.1 Detaching test (failure load)

The detachment failure loads for each material at 4, 8, 16, and 26 weeks after implantation are summarized in Fig. 3. The failure loads for the UT-GM, ACaH-GM, ACaHW-GM and AH-Ti groups were, respectively, 0 ± 0, 0.863 ± 1.496, 8.95 ± 5.829, and 6.463 ± 4.786 N at 4 weeks; 0 ± 0, 2.25 ± 3.053, 16.138 ± 10.182, and 19.988 ± 9.547 N at 8 weeks; 0 ± 0, 2.7 ± 2.882, 19.988 ± 13.868, and 25.05 ± 13.302 N at 16 weeks; and 0 ± 0, 3.563 ± 2.488, 20.55 ± 13.741, and 27.9 ± 10.890 N at 26 weeks. The UT-GM group showed a failure load of 0 N at all times, while the ACaH-GM group showed a slight increase in failure load throughout the experimental period. In contrast, at all time periods, both the ACaHW-GM and AH-Ti samples showed statistically significant higher failure loads than those of UT-GM and ACaH-GM groups (for *P* values, please see the figure caption). At all periods of the study, no statistically significant differences in failure loads between the ACaHW-GM and the AH-Ti groups were found ($P = 0.835$ at 4 weeks, $P = 0.6219$ at 8 weeks, $P = 0.8601$ at 16 weeks and $P = 0.5547$ at 26 weeks). The failure loads for all groups (apart from the UT-GM samples) increased steadily with time.

3.2.2 Histological examination

3.2.2.1 Surface examination after detaching tests After the detaching tests, bone residue was observed on the intact surface layer of the treated plates in SEM images taken at all time intervals. From SEM–EDX analysis, the bony areas had more Ca than the $CaCl_2$-treated metal surfaces, and also contained *P*, while Ti was only present at the metal surface, so we could easily distinguish the bony area from the metal surface. In the images taken at 4 weeks, there was little bone residue on ACaH-GM plates. These plates showed almost no increase in bone residue throughout the experimental period. From 4 weeks to 26 weeks, there was no bone residue on all UT-GM plates. In contrast, some bone residue was observed on the ACaHW-GM (Fig. 4a) and AH-Ti plates at 4 weeks, and the amount of residue increased with time. Bone tissue was well integrated on the ACaHW-GM and AH-Ti plates at all time periods. At 26 weeks, we observed abundant integration of bone tissue on the ACaHW-GM (Fig. 4b) and AH-Ti plates, and the visible areas of metal surface were decreased. Consistent with this finding, no Ti was observed (nor detected by EDX) on the bony surfaces after detaching tests for the ACaHW-GM and AH-Ti samples, indicating that the treated surface structure is sufficiently strong.

3.2.2.2 Histological examination Representative histological images for each sample group are shown in Fig. 5 (at 4 weeks) and Fig. 6 (at 26 weeks). In the samples from the ACaHW-GM and AH-Ti groups, new bone (NB) had formed in the gap at the implantation site within 4 weeks, and a large amount of new bone was in contact with the surface (Fig. 5c, d). The samples from the UT-GM and ACaH-GM groups had an intervening layer of soft tissue between the bone and the implant at 4 weeks (Fig. 5a, b).

At 26 weeks, the newly formed bone had become remodeled and exhibited more organized collagen patterns in all samples; however, the amount of bone was far greater in the samples from the ACaHW-GM and AH-Ti groups than in the samples from the UT-GM and ACaH-GM groups (Fig. 6). These histological findings were consistent with the results of mechanical testing.

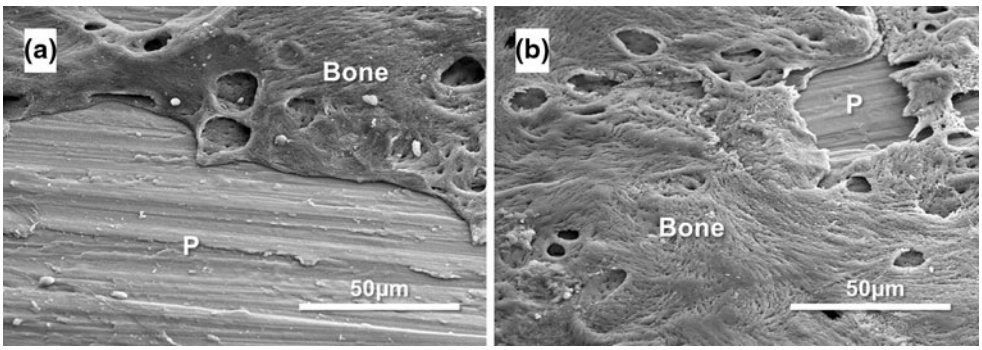

Fig. 4 SEM images of the surface of an ACaHW-GM plate after detaching tests at (**a**) 4 weeks and (**b**) 26 weeks. (**a**) Some bone residue (Bone) was observed on the ACaHW-GM plate (P) at 4 weeks. (**b**) Much more bone residue (Bone) was observed on the ACaHW-GM plate (P) at 26 weeks

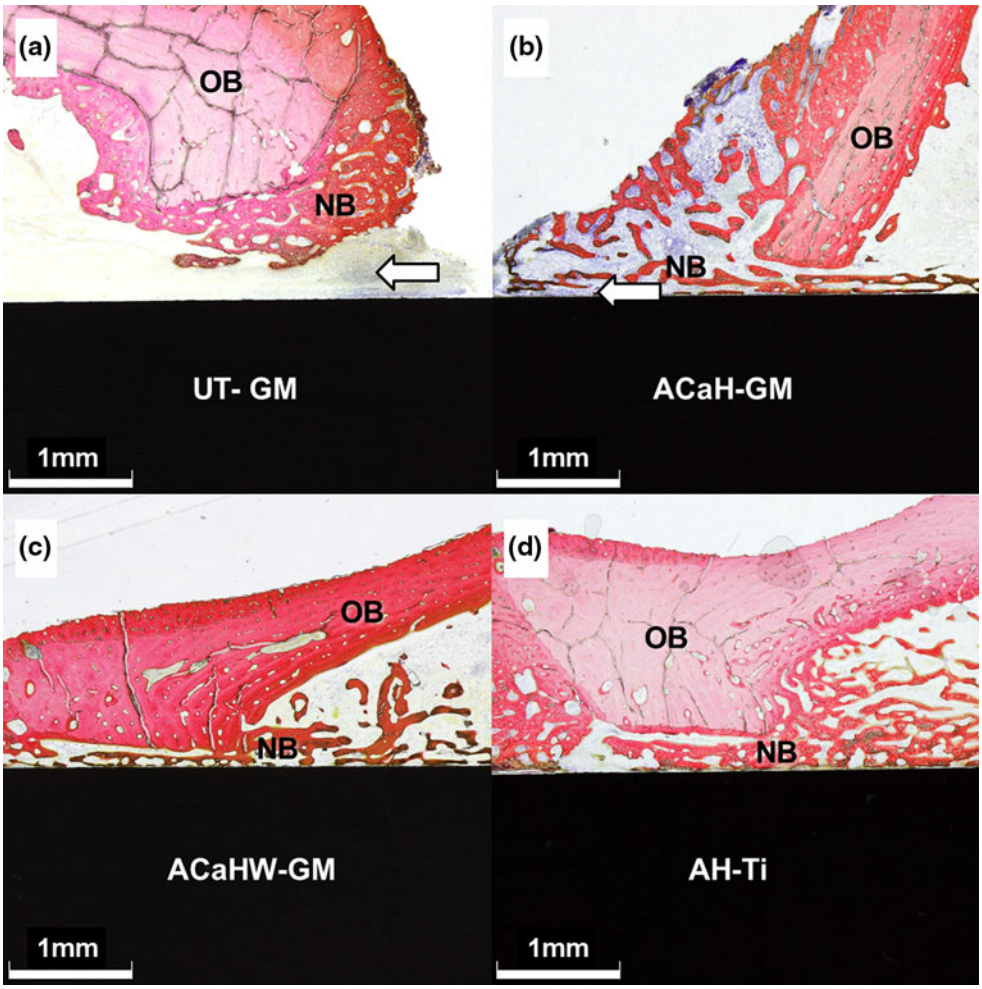

Fig. 5 Surface staining of the bone–implant interface with Stevenel's blue and Van Gieson's picrofuchsin at 4 weeks. (**a**) UT-GM, (**b**) ACaH-GM, (**c**) ACaHW-GM, and (**d**) AH-Ti. *OB* original bone; *NB* new bone. *White arrows* indicate a gap between the plate and new bone

4 Discussion

ACaHW-GM successfully bonded to bone and retained this bond for up to 26 weeks; its performance was similar to that of AH-Ti, which is already known to be bioactive. In contrast, the UT-GM and ACaH-GM showed almost no bonding until 26 weeks. Histological examination confirmed that the newly formed bone tissue made direct contact with the ACaHW-GM and AH-Ti implants as early as 4 weeks after surgery. Conversely, for the UT-GM and

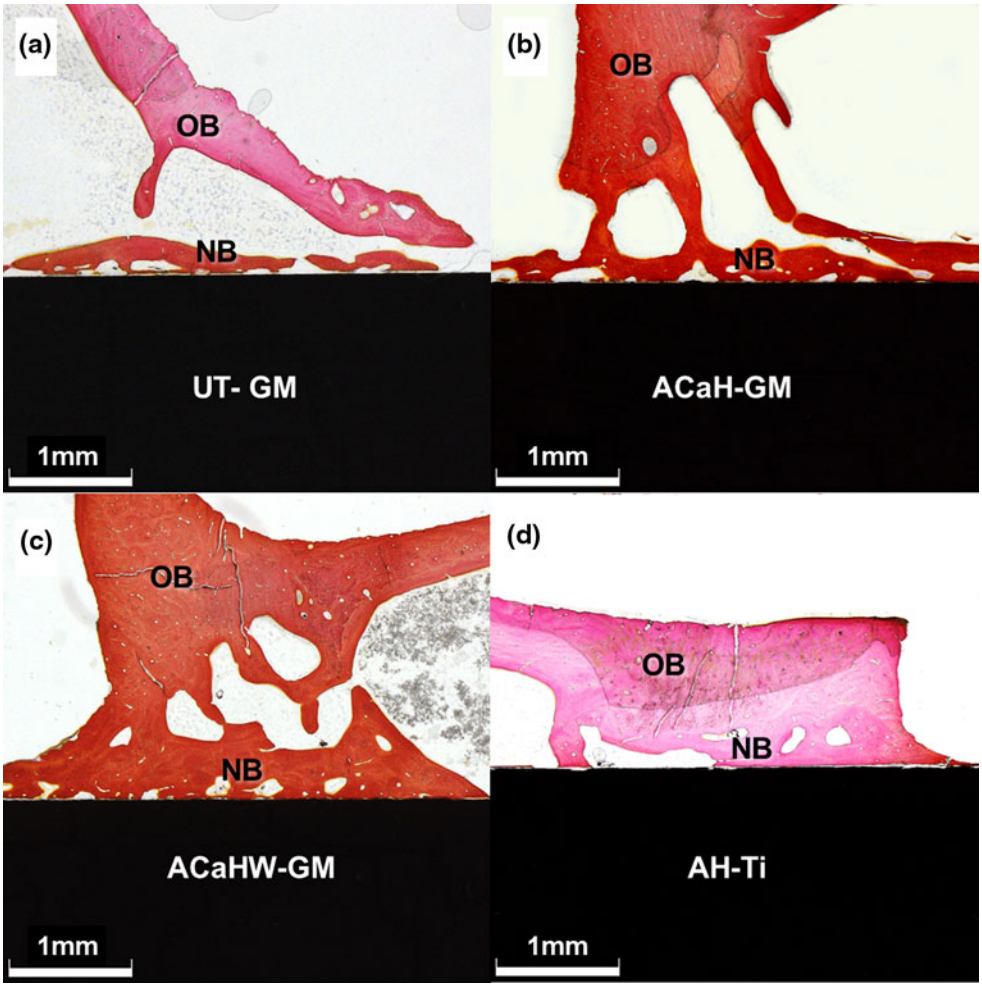

Fig. 6 Surface staining of the bone–implant interface with Stevenel's blue and Van Gieson's picrofuchsin at 26 weeks. (**a**) UT-GM, (**b**) ACaH-GM, (**c**) ACaHW-GM, and (**d**) AH-Ti. *OB* original bone; *NB* new bone

ACaH-GM samples, a layer of fibrous tissue existed at the bone–implant interface 8 weeks after surgery, and the bone tissue made only partial contact with the implant at 16 and 26 weeks. These results confirm that ACaHW treatment of gum metal enhanced its bone-bonding ability.

Both ACaHW-GM and ACaH-GM have nanometer-scale fine network structures on their surfaces (Fig. 2b, c). However, the failure load of ACaHW-GM was higher than that of ACaH-GM at all time periods. This means the bioactivity of gum metals cannot be attributed to their surface structures. In previous studies, the surfaces of ACaHW-GM showed apatite-forming abilities when soaked in SBF for 3 days; this behavior was not seen for the ACaH-GM plates [11]. It has been shown that Ti and Ti-based alloys with surfaces conducive to apatite formation in SBF bond to living bone through the apatite layer that forms on their surfaces in the living body [12–14]. These findings suggest that it is the apatite-forming ability of the ACaHW-GM samples that enables them to tightly bond to living bone in the body.

We suggest that apatite forms on the surfaces of ACaHW-GM samples but not on ACaH-GM samples, because of differences in chemistry. When the gum metal is subjected to $CaCl_2$ treatment after NaOH treatment, the calcium ions can substitute for sodium in the sodium hydrogen titanate formed by the NaOH treatment; the result of this is a layered calcium hydrogen titanate structure, $Ca_xH_{2-2x}Ti_3O_7$, on the surface. This calcium hydrogen titanate is then transformed into various forms of calcium titanate (such as $CaTi_4O_9$, $CaTi_2O_4$, and $CaTi_2O_5$), calcium niobate (such as $Ca_2Nb_2O_7$ and $CaNb_2O_6$), rutile, and anatase by the subsequent heat treatment. The gum metal treated to this point did not show apatite-forming ability in SBF, probably because of the extremely slow diffusion of calcium ions from the calcium titanates and niobates, as has been previously seen for the calcium titanate formed on the surface of Ti–15Zr–4Nb–4Ta

alloy [20]. The final water treatment step results in some of the calcium ions in the surface layer being exchanged for oxonium ions, without an apparent change in the crystal phases. Thus, the resultant phases can be described as $Ca_xH_{2-2x}Ti_4O_9$, $Ca_xH_{2-2x}Ti_2O_4$, and $Ca_xH_{2-2x}Ti_2O_5$ for the calcium-deficient calcium titanate, and $Ca_xH_{4-2x}Nb_2O_7$ and $Ca_xH_{2-2x}Nb_2O_6$ for the calcium-deficient calcium niobate. The gum metal treated in this way (the ACaHW-GM samples) exhibited a high capacity for apatite formation in SBF probably because of the increased mobility of the calcium ions in the calcium titanates and niobates caused by incorporation of the oxonium ions [11].

In our animal study, the ACaHW-GM samples showed good affinity for bone tissue, and histological examinations demonstrated biocompatibility. The ACaHW-GM plate, which is V-free Ti alloy, seems to be nontoxic with good osteoconductivity.

To resolve stress shielding after cementless total hip arthroplasties, which can arise because of differences in Young's modulus between the stem and human cortical bone, the Young's modulus of the alloy used for the stem alloy needs to be close to the Young's modulus of human cortical bone [7–9]. To precisely assess local stress–strain distributions in geometrically complex structures, finite element methods are a standard tool used in biomedical engineering [21]. A finite element model (FEM) of a biomimetic stem (composed of hydroxyapatite–coated carbon fibers), with material properties similar to those of a cortical bone (Young's modulus is 5–30 GPa) was constructed [22]. Three static load cases representing slow walking, stair climbing, and gait in a healthy individual were considered. Stress shielding was evaluated and compared with the results of a similar FEM for a titanium alloy (Ti–6Al–4V). The composite stems allowed for reduced stress shielding when compared with a traditional Ti–6Al–4V stem.

The Young's modulus of the gum metal used in this study is 55 GPa, much closer to that of human cortical bone (10–30 GPa) than Ti–6Al–4V alloy (110 GPa), so the gum metal should reduce stress shielding in the femur, and thus decrease thigh pain. Further animal studies and FEM analyses are needed to test this hypothesis.

Thus, ACaHW-GM should be useful for developing novel orthopedic implants such as cementless joint replacements or dental implants, because of its good bone bonding ability. The gum metal should also prevent stress shielding under loaded conditions because it has a low Young's modulus.

5 Conclusions

A gum metal with composition Ti–36Nb–2Ta–3Zr–0.3O exhibited bone bonding ability in vivo after successive NaOH, $CaCl_2$, heat (700 °C), and water treatments. The present results suggest that the gum metal may be useful in novel orthopedic implants or dental implants because of its excellent bioactivity. The low Young's modulus of gum metal mean that stress shielding under loaded conditions should be able to be prevented.

References

1. Niinomi M, Hattori T, Morikawa K, Kasuga T, Suzuki A, Fukui H, et al. Development of low rigidity β-type titanium alloy for biomedical applications. Mater Trans. 2002;43(12):2970–7.
2. Head WC, Bauk DJ, Emerson RH Jr. Titanium as the material of choice for cementless femoral components in total hip arthroplasty. Clin Orthop Relat Res. 1995;311:85–90.
3. Long M, Rack HJ. Titanium alloys in total joint replacement–a materials science perspective. Biomaterials. 1998;19(18):1621–39.
4. Mont MA, Hungerford DS. Proximally coated ingrowth prostheses. A review. Clin Orthop Relat Res. 1997;344:139–49.
5. Nourbash PS, Paprosky WG. Cementless femoral design concerns. Rationale for extensive porous coating. Clin Orthop Relat Res. 1998;355:189–99.
6. Glassman AH, Bobyn JD, Tanzer M. New femoral designs: do they influence stress shielding? Clin Orthop Relat Res. 2006;453:64–74.
7. Andrew TA, Flanagan JP, Gerundini M, Bombelli R. The isoelastic, noncemented total hip arthroplasty. Preliminary experience with 400 cases. Clin Orthop Relat Res. 1986;206:127–38.
8. Butel J, Robb JE. The isoelastic hip prosthesis followed for 5 years. Acta Orthop Scand. 1988;59(3):258–62.
9. Niinimaki T, Jalovaara P. Bone loss from the proximal femur after arthroplasty with an isoelastic femoral stem. BMD measurements in 25 patients after 9 years. Acta Orthop Scand. 1995;66(4):347–51.
10. Saito T, Furuta T, Hwang JH, Kuramoto S, Nishino K, Suzuki N, et al. Multifunctional alloys obtained via a dislocation-free plastic deformation mechanism. Science. 2003;300(5618):464–7. doi:10.1126/science.1081957.
11. Yamaguchi S, Kizuki T, Takadama H, Matsushita T, Nakamura T, Kokubo T. Formation of a bioactive calcium titanate layer on gum metal by chemical treatment. J Mater Sci - Mater Med. 2012;23(4):873–83. doi:10.1007/s10856-012-4569-7.
12. Nishiguchi S, Kato H, Fujita H, Kim HM, Miyaji F, Kokubo T, et al. Enhancement of bone-bonding strengths of titanium alloy implants by alkali and heat treatments. J Biomed Mater Res. 1999;48(5):689–96.
13. Kim HM, Miyaji F, Kokubo T, Nakamura T. Preparation of bioactive Ti and its alloys via simple chemical surface treatment. J Biomed Mater Res. 1996;32(3):409–17. doi:10.1002/(SICI)1097-4636(199611)32:3<409:AID-JBM14>3.0.CO;2-B.
14. Fukuda A, Takemoto M, Saito T, Fujibayashi S, Neo M, Yamaguchi S, et al. Bone bonding bioactivity of Ti metal and Ti-Zr-Nb-Ta alloys with Ca ions incorporated on their surfaces by simple chemical and heat treatments. Acta Biomater. 2011;7(3):1379–86. doi:10.1016/j.actbio.2010.09.026.
15. Niinomi M. Recent metallic materials for biomedical applications. Metall and Mat Trans A. 2002;33(3):477–86. doi:10.1007/s11661-002-0109-2.
16. Kim HM, Miyaji F, Kokubo T, Nakamura T. Effect of heat treatment on apatite-forming ability of Ti metal induced by alkali treatment. J Mater Sci - Mater Med. 1997;8(6):341–7.
17. Nishiguchi S, Nakamura T, Kobayashi M, Kim HM, Miyaji F, Kokubo T. The effect of heat treatment on bone-bonding ability of alkali-treated titanium. Biomaterials. 1999;20(5):491–500.

18. Fujibayashi S, Nakamura T, Nishiguchi S, Tamura J, Uchida M, Kim HM, et al. Bioactive titanium: effect of sodium removal on the bone-bonding ability of bioactive titanium prepared by alkali and heat treatment. J Biomed Mater Res. 2001;56(4):562–70.
19. Nakamura T, Yamamuro T, Higashi S, Kokubo T, Itoo S. A new glass–ceramic for bone replacement: evaluation of its bonding to bone tissue. J Biomed Mater Res. 1985;19(6):685–98. doi:10.1002/jbm.820190608.
20. Yamaguchi S, Takadama H, Matsushita T, Nakamura T, Kokubo T. Apatite-forming ability of Ti–15Zr–4Nb–4Ta alloy induced by calcium solution treatment. J Mater Sci - Mater Med. 2010;21(2):439–44. doi:10.1007/s10856-009-3904-0.
21. Sakai R, Itoman M, Mabuchi K. Assessments of different kinds of stems by experiments and FEM analysis: appropriate stress distribution on a hip prosthesis. Clin. Biomech. (Bristol, Avon). 2006;21(8):826–33. doi:10.1016/j.clinbiomech.2006.03.008.
22. Caouette C, Yahia L, Bureau MN. Reduced stress shielding with limited micromotions using a carbon fibre composite biomimetic hip stem: a finite element model. Proc Inst Mech Eng [H]. 2011;225(9):907–19. doi:10.1177/0954411911412465.